Al-Qadisiyah Journal for Engineering Sciences 15 (2022) 067–072

Contents lists available at http://qu.edu.iq

Al-Qadisiyah Journal for Engineering Sciences

Journal homepage: http://qu.edu.iq/journaleng/index.php/JQES

# Studying the effect of multicomponent nano-coating alloy on hydrogen embrittlement of AISI 1018 steel by gas-phase process

***Zainab Z. Ali*, Baha S. Mahdi and Ameen D. Althamer***

*Production and Metallurgy Department, University of Technology, Baghdad, Iraq.*

ARTICLE INFO

Article history:
Received 26 October 2021
Received in revised form 25 January 2022
Accepted 18 March 2022

*Keywords:*
Hydrogen embrittlement
Tensile test
DC sputtering
BNi-2
*SEM.*

ABSTRACT

The present study is attempted to investigate the influence of multicomponent Ni-alloy (BNi-2) on the hydrogen embrittlement (HE) behaviour of AISI 1018 steel by using cathodic protection and tensile test. The results show that the HE indexes (HEI) decrease notably when AISI 1018 steel is coated with BNi-2 alloy by DC sputtering process. This coating processes leads to decrease in HE susceptibility of the AISI 1018 steel, which can be rationalized to the enhancement in corrosion resistance and the decrease in hydrogen absorption of the AISI 1018 steel after coating. The tensile strengths of bared samples were decreased with increasing charging time until 24 hours when stable at values 350 MPa. while the coated samples showed an increasement in the tensile strength from 570 MPa to 750 MPa. stabilization in strength at value of 600 MPa was observed after exceeding 48 hours. Also, the tensile test for uncoated specimens indicated a clear reduction on the modulus of elasticity compared with other coated ones.

© 2022 University of Al-Qadisiyah. All rights reserved.

## 1. Introduction

The deterioration effect of hydrogen penetration on steel properties have been observed since 1870s, Johnson noted the changes in the toughness and breaking strain of iron, when it was temporarily immersed in acid for just a few minutes. The acids which produce the hydrogen during the reaction with iron lead to a serious deterioration in properties. [1]. Rates of hydrogen diffusion in metals depend on the hydrogen concentration gradient, temperature, stress, susceptible materials, hydrogen-diffusion coefficients (D) and the crystal structure [2]. For example, high-strength martensitic steels are so susceptible to hydrogen penetration, since cracks are observed at solute hydrogen concentrations less than 1 ppm (wt.). For ferritic steels with strengths less than 750 MPa, relatively high hydrogen concentrations (~10 ppm) are often necessary for the hydrogen penetration to be significant. Nickel alloys, alumina, stainless steels, and copper alloys show little susceptibility to hydrogen penetration; Fig. 1, [2-3]. The main sources of hydrogen can be summarized as cathodic protection, pickling, electroplating, special case of arc welding, galvanic corrosion, and acid or gasses chemical reactions [4]. Hydrogen penetration weakens the interatomic bonds between the grains of steel casing and causes premature failures. This phenomenon could pose a risk to the sustainability of the oil and gas projects. Therefore, nano-coatings were used to treat this problem. Nanocoating term is used if the coating thickness is referred to as thin films or the structures are in nanostructure scales. There are various methods of producing nano-coatings, thin films, and nanostructure [5], which are chemical vapor deposition (CVD) and physical vapor deposition (PVD). The Phase structure, morphology, and mechanical properties of coatings deposited using DC.

* *Corresponding author.*
E-mail address: *pme.19.38@grad.uotechnology.edu.iq* (Zainab Ali)

https://doi.org/10.30772/qjes.v15i1.815
2411-7773/© 2022 University of Al-Qadisiyah. All rights reserved. *This work is licensed under a Creative Commons Attribution 4.0 International License.*

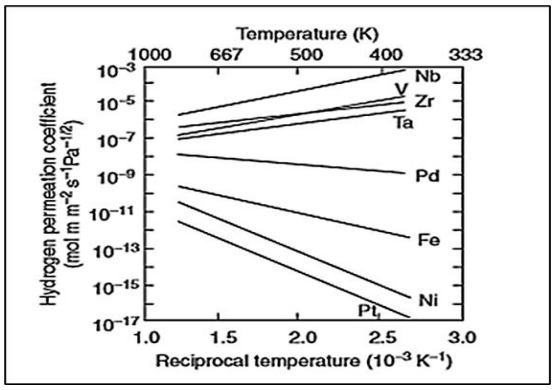


**Figure 1. Hydrogen diffusion coefficients for Fe and Nb (bcc), Ni (fcc) and Ti (hcp) as a function of temperature [2] [3]**

Such as type of inert gas, working pressure, voltage, deposition time, substrate temperature, the distance between target and substrate, the surface finish of substrate, ion current, etc. [6] [7] [8]. They are directly affecting phase structure, preferred orientation, chemical composition, and deposition rate of the coatings [9] [10] Several researchers revealed the effect of nanocoating on hydrogen penetration and corrosion resistance for steel. S. Marikkannu and others reported that Indium oxide $In_2O_3$ nano coating deposited films are successfully deposited on different substrates by using the gas phase process, the results are encouraging for the use of thin films in low-cost industry applications [11].

BNi-2 alloy has been used in applications in environments withstanding temperatures up to 1,000 °C, with properties that include abrasion resistance to guard against erosion, kinetics that makes it impervious to atomic hydrogen penetration and ingress can cause steel to become brittle and crack. This work focuses on reducing the hydrogen embrittlement in AISI 1018 steel by coating processes. Multicomponent nano-coating alloy BNi-2 as protective films will be deposited by using DC sputtering technique.

## 2. Material and experimental setup

### 2.1. Materials used

Steel (AISI 1018), which is used in oil industry storage tanks, is used as a substrate material exposed to hydrogen charging with and without coating. The chemical composition analysis of this workpiece was done by using spectrometer analysis instrument available in Baghdad in the General Company for Examination and Rehabilitation Engineering, as shown in Table 1.

**Table 1. Chemical composition of test specimen (in %).**

| Elem. | C | Si | Mn | Cr | Mo | Ni | Co | Cu | Nb | Fe |
|---|---|---|---|---|---|---|---|---|---|---|
| wt% | 0.18 | 0.22 | 0.75 | 0.09 | 0.02 | 0.12 | 0.03 | 0.03 | 0.02 | Rest |

Thin film deposition has been obtained via DC or Direct Current Sputtering. The target material used was the foil of nickel alloy called BNi-2 or (EN ISO 17642). The thickness of this foil was 35 mm and its chemical composition are explained in table (2) [12].

**Table 2. Chemical composition of target foil (BNi-2).**

| Elem. | Cr | B | P | Si | Fe | C | Ni |
|---|---|---|---|---|---|---|---|
| wt% | 14 | 3 | 0.02 | 4.2 | 3 | 0.04 | Rest |

### 2.2. Specimen preparation

Surface preparation of substrate samples was carried out by emery papers of silicon carbides with different grit sizes from 220, 400, 800, and 1000. The samples also were ultrasonically cleaned in ethanol for 15 min prior to the deposition process.

### 2.3 Coating process

Coating process was performed by DC sputtering, where the nickel alloy foil was prepared as a circular target with a diameter of 50 mm and fixed 2.5 centimeters above the substrate of specimens. The chamber was evacuated partially to a pressure of $10^{-1}$ mbar of pure Argon gas. The target was bombarded with ionized Argon gas molecules causing atoms to be "Sputtered" off into the plasma. These took off atoms then deposited when they condensed as a thin film on the substrate to be coated. Adjusted DC sputtering for coating thin-film current was 16 mA and the sputtering time was fixed for all specimens to 50 minutes.

### 2.4 Effect of Hydrogen Embrittlement (HE):

Firstly, the dog bone-shaped (tensile) specimens of mild steel were welded to one end of a copper wire by discharge welding, and then the other end of the wire was connected to the cathode wire of the power supply. The tensile specimens were covered with an acid-resistant insulating material (epoxy) except the gauge length remained uncoated, and the uncoated area calculated for specimens was about 250 $mm^2$, as shown in figure -3-. The anode was a stainless-steel bar.

**Figure 2. Coated and uncoated work substrate before covering**

Sulfuric acid ($H_2SO_4$) dissolved in distilled water with a concentration of 0.5 M was used to create hydrogen-releasing environments. The test specimens were immersed in $H_2SO_4$ solutions in a beaker. For better understanding and statistical analysis of hydrogen damage, ten specimens were immersed in each of $H_2SO_4$ solutions, a half of them were coated and the other not; they were immersed for different intervals of time (2, 4, 6, 24, and 48 hours). The power supply was adjusted with 0.3 v and the average current was 0.4 A with a current density of 120 mA/cm$^2$.

**Figure 3. Partially covered tensile test specimens by epoxy resin**

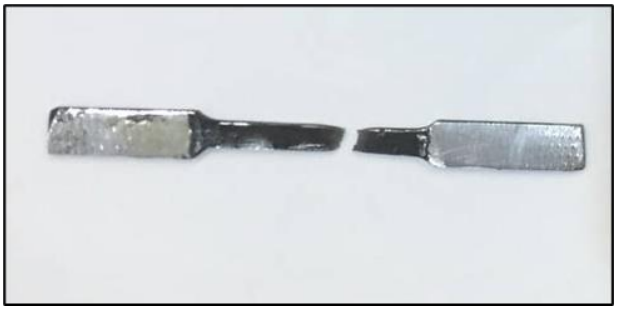

**Figure 4. Specimen failed after tensile test.**

**2.5. machining testing**

Tensile test specimens were prepared according to ASTM E8 with a gage length of 25 mm, and the total length for each specimen was 100 mm. The machining process for all specimens was done using a CNC machine, as shown in Fig. 2.

**2.6. Morphology analysis**

Coated and charged samples with dimension (10×10) mm were prepared to test using SEM. Figure 5 shows the coated AISI 1018 steel with BNi-2 alloy, where the scratched surface belongs to the prior grinding process. From the image, the coating layer completely covers the steel surface.

**3. Results and discussions**

**3.1 Hydrogen Penetration:**

Standard tensile specimens of AISI 1018 steel were charged with hydrogen, the specimens were tested by a tensile test at the room temperature, and the results are shown in Fig. 5.

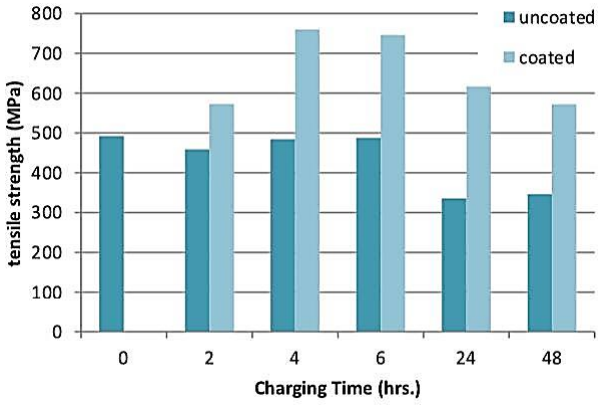


**Figure 5. A graph illustrating the results of all tensile tested specimens**

The first impression of the tested specimens is that the uncharged sample will give the maximum tensile strength as it is known, in this experiment it reached to 490 MPa, where the uncharged specimen is free of side effects of hydrogen penetration defects. Also, all the charged specimens will suffer from defects according to charging time and this is also applied to the coated specimens, where the coat has not blocked all the hydrogen atoms but it can reduce the penetration. In Fig. 5, the result is different from what was expected. Charging the uncoated specimens give the expected results as mentioned above by decreasing the tensile strength for all the uncoated specimens but at different values when compared to the charging time.

Fitting curve for uncoated specimens as depicted in Fig. 6 has been done to understand the relation between tensile strength as mechanical properties and hydrogen charging. As it is expected, the uncoated specimens evince a decrease in tensile strength with longer charging time until reaching a steady state value about 30% of the original uncharged metal after 24 hours of immersion in dilute sulfuric acid. In the actual embedded pipelines in sites, the same happened but for a longer time depending on the cathodic current density, soil type, and humidity. Nearest curve fitting is the second order polynomial formula as stated in Eq. 1, where $\sigma_u$ is the tensile strength in MPa, and T is the charging time in hours. Note that this equation is applied for a specific environment involved in this work.

By curve fitting, the sputtered tensile charged specimens illustrated Fig. 7 showed the unexpected behavior, where the tensile strength increased above the uncharged steel for just nano coating thickness. And, Eq. 2 represents the second-order polynomial curve fitting, the increasing percentage value can be 24% which is very high, and it is noted that this happened without heat treatment.

$$\sigma_u = 503 - 9.299T - 0.124T^2 \quad (1)$$

$$\sigma_u = 405 - 29.3T - 0.556T^2 \quad (2)$$

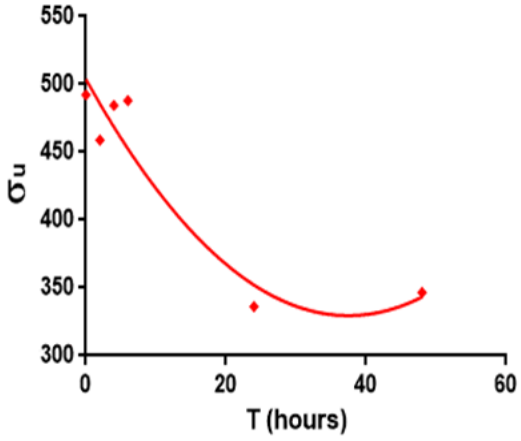


**Figure 6. Tensile strength for uncoated specimens with different charging times.**

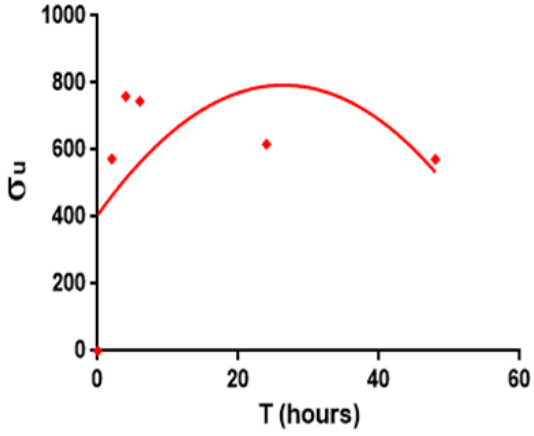


**Figure 7. Tensile strength for coated specimens with different charging times.**

By curve fitting, the sputtered tensile charged specimens illustrated in Fiq. 7 showed the unexpected behavior, where the tensile strength increased above the uncharged steel for just nano-coating thickness. Eq. 2 denotes the fitting of a second-order polynomial curve. the increasing percentage value can be 24% which is very high, and it is noted that this happened without heat treatment.

Increasing tensile strength in coated and charged hydrogen specimens necessitates additional tests such as TEM, which are not included in this study. However, there are several explanations for this phenomenon, the first of which is the entrance of the coating elements into the base metal via a diffusion process aided by the high energy of hydrogen. These elements react with iron and form strain hardening inside metal, finally the occurrence of phase transformations. But this explanation is weak because the coating elements as nickel, chromium and others are hard to diffuse substitutionally at room temperature.

The second explanation is that the BNi-2 nano-coating layer on steel could heal most nano and micro cracks in the substrate surface and reduce the stress concentrations, causing improved mechanical properties [13].

The third explanation which needs good attention and is the nearest to be approved is that the nano coating layer acts as a sieve for the hydrogen atoms, which means the coating allows the hydrogen atoms to pass into the structure in a small amount. Therefore, they are distributed within the crystal lattice in a uniform and homogeneous manner. Hydrogen atoms occupy interstitial sites within the crystal lattice, leading to a distortion in it (Because the space inside the lattice is not enough to accommodate a solute atom without the displacement of neighboring atoms). This distortion is the tension and compression energy between the iron and hydrogen atoms inside the metal, where the crystal structure is stable and the distance between the iron atoms are fixed. So, when the hydrogen atoms enter, the iron atoms move away from each other; thus, the tensile and compressive forces are generated, and it looks like cold work inside the metal [14].

### 3.2 SEM analysis and finding the thickness:

Figure 8 seems that it is not completely uniform as there are some scratches like a terrace, this is due to surface finish, and this is because of the nature of the sputtering process which requires some roughness to increase the surface area and mechanical interlocking between the coating atoms and substrate. It is clear that these terraces are formed by the stacking of layered crystals. On the other hand, roughness is required to reduce the hydrogen blistering as concluded by several researchers. The grinded surface presents a lower sensitivity to the hydrogen-induced blisters in comparison with the polished surface, which is attributed to the suppression of hydrogen invasion caused by higher residual compressive stress and higher dislocation density in the grinded surface [15].

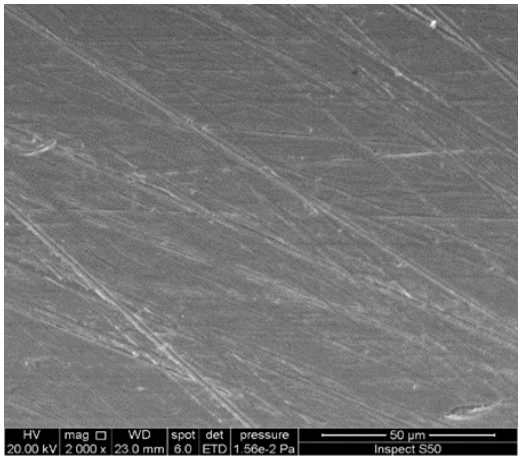


**Figure 8. SEM image for coated surface with low magnification**

To identify the thickness of the nanolayer, the best method is by scratching the coated surface using a sharp razer smoothly. By increasing the magnification, the scratch becomes clearer, and the white marked region represents the accumulated coating layer of BNi-2, as shown in Fig. 9. To recognize the layer thickness, the magnification must be higher. With higher magnification and lower beam intensity (4 mA) for the electron beam, the segmented separated coating layers from the surface can be seen, as portrayed in Fig. 10. Thin fragmented layer parts are shown in Fig. 10 as

semi-transparent to electron beam as marked some of them by dotted yellow lines to make better vision.

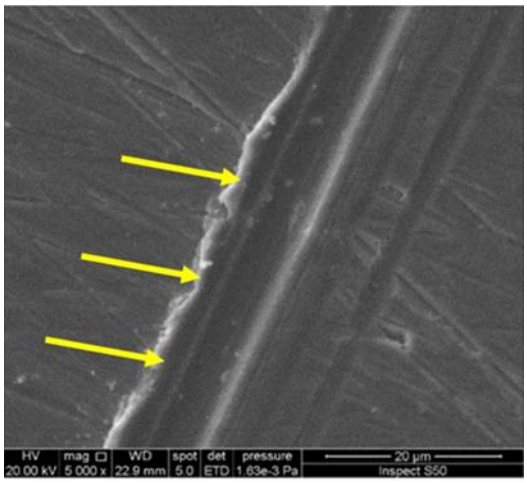


**Figure 9. SEM image for scratched surface using sharp razer**

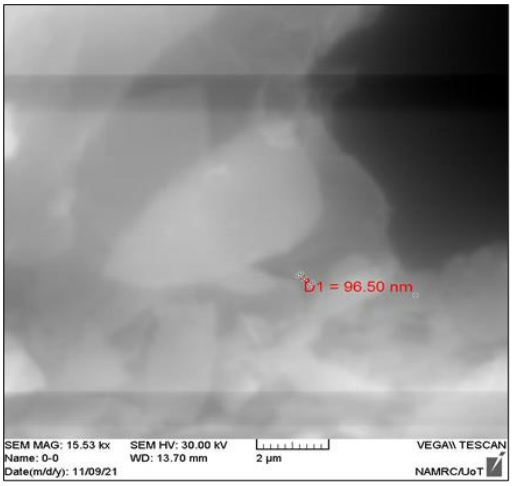


**Figure 10. SEM image for the scratched surface in figure (10) with higher magnification.**

To confirm the thickness result, another image with a higher magnification was taken as shown in Fig. 11, where the measured thickness was 114.56 nm. According to the above, one can say that the coat layer thickness lies between (90 to 110) nm, and it can be classified as nano or thin layer. Fig. 12 displays the SEM image with low magnification for coated charged samples, and it is observed that there are different areas of the inhomogeneous samples. In this figure, the microcracks, and ripping of coating from small areas, as well as some spots, can be seen; this means that the hydrogen atoms began to slightly and regularly penetrate the coating layer. Coating microstructure plays an important role in affecting mechanical and tribological properties as well as hydrogen permeation, since the nickel structure (FCC), is a better metallic coating type for resisting the hydrogen penetration than (BCC) elements because the packing factor of (FCC) is more than the (BCC) structure related to fewer voids between atoms in (FCC) compared to the (BCC) crystal lattice. Therefore, the hydrogen atoms cannot easily penetrate throughout the structure, and that is happened in this sample. The surface roughness values for coated, uncoated, and charged specimens are measured by using a roughness device, and the results were as follows. The substrate roughness before coating and before the charging process was found to be equal to 0.1466 µm, coated uncharged steel equal to 0.093 µm, and Coated glass was 0.04 µm. The roughness that appeared in the steel-coated layer is related to the steel surface itself and is not due to the sputtering process as in Fig. 13 showing the glass coated with the same amount (time and other parameters) for steel. The smoothness of the coated glass is higher in orders compared to the coated steel surface. When comparing Figs. 8-13, one can notice clearly the homogeneity of lass rather than metal substrate, because the tops and valleys in metal substrate act as nuclei which collect the sputtered atoms, but that does not exist in a glass. This is the reason for different images in metal and glass substrates.

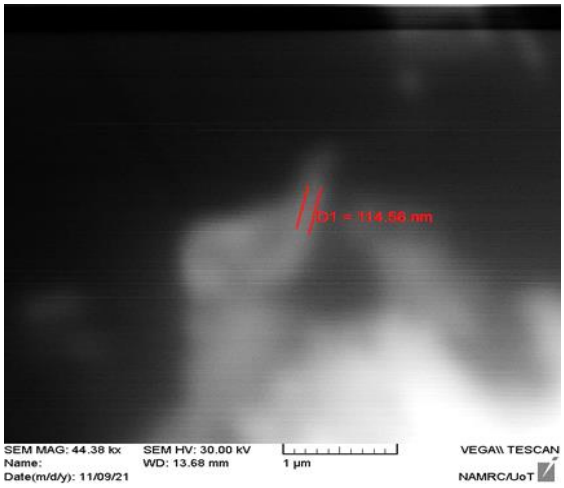


**Figure 11. High magnification SEM images show measurement of nano sputtering layer.**

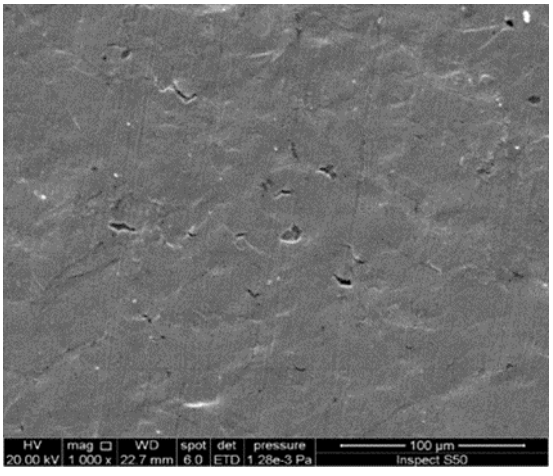


**Figure 12. SEM images of BNi-2 deposited on metal with HE.**

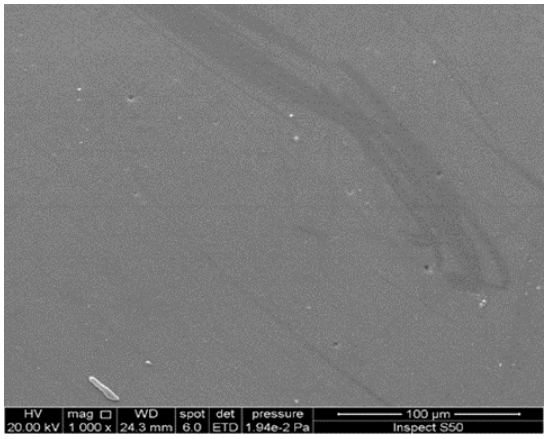


**Figure 13. SEM image of the BNi-2 deposited on glass.**

## 4. Conclusions

1) Uncoated AISI 1018 steel and charged by hydrogen manifested a decrease in tensile strength until a steady state about 30% of its original tensile strength after a charging time of 24 hours with a current the density of 120 mA/cm$^2$.
2) Increasing the tensile strength by 24% to the original metal by hydrogen charging for BNi-2 nanolayer on the AISI 1018 steel.
3) Most suggested cause of increasing the tensile strength by hydrogen charging for the coated metal is the action of the nano-coating layer as a sieve for the diffused hydrogen atoms distributed interstitially between the iron atoms, leading to stress in the lattice as occurring in the cold work strengthening.
4) Average coat thickness of BNi-2 on AISI 1018 Steel was 90 to 100 nm and the maximum coat layer was 114.5 nm.

## REFERENCES

[1] W. H. Johnson, Proceedings of the Royal Society of London, p. 168–179., 23 (1875).

[2] J Völkl and G. Alefeld, "Hydrogen diffusion in metals," in Diffusion in Solids, p. 231–302, 1975.

[3] M. D. a. S. Z. H.-J. Christ, "Hydrogen diffusion coefficients in the titanium alloys IMI 834, Ti 10–2–3, Ti 21 S, and alloy C, Metal," pp. 1507–1517, 2000.

[4] s. lynch, "Hydrogen embrittlement (HE) phenomena and mechanisms," in Stress Corrosion Cracking, Australia, 2011, pp. 90-130.

[5] a. L. B. Injeti G., "“Electrodeposition of nanostructured coatings and their characterization”," J. of Science and Technology of Advanced materials, pp. 121-129, 2008.

[6] B. Warcholinski and A. Gilewicz, " Effect of substrate bias voltage on the properties of CrCN and CrN coatings deposited by cathodic arc evaporation.," Vols. 90, p. 145–150., 2013.

[7] A. Obrosov, M. Naveed, A. Volinsky and S. Weiß, " Substrate frequency effects on CrxN coatings deposited by DC magnetron sputtering.," Vols. 26, p. 366–373., 2017.

[8] A. Krella and A. Czyzniewski, "Cavitation resistance of Cr-N coatings deposited on austenitic stainless steel at various temperatures.," Vols. 266, p. 800–809, 2009.

[9] X. Wan, S. Zhao, Y. Yang, J. Gong and C. Sun, " Effects of nitrogen pressure and pulse bias voltage on the properties of Cr-N coatings deposited by arc ion plating.," Surf. Coat. Technol., Vols. 204, p. 1800–1810, 2010.

[10] H. Shah, R. Jayaganthan and D. Kaur, " Effect of sputtering pressure and temperature on dc magnetron sputtered CrN films," Vols. 26, p. 629–637, 2010.

[11] M. K. A. A. S. MARIKKANNU, "STUDIES ON JET NEBULISER PYROLYSED INDIUM OXIDE THIN FILMS," Journal of Ovonic Research, vol. 10, pp. pp. 115 - 125, August 2014.

[12] Metals Handbook, " Properties and Selection nonferrous," in ASM, 2015, pp. p1832.

[13] K. N., J.-M. Y., J. K. Tamaki Naganuma, "The effect of a compliant polyimide nanocoating on the tensile properties of a high strength PAN-based carbon fiber," composites science and technology, 2009.

[14] Underneath the Bragg Peaks – Structural Analysis of Complex Materials, vol. 16, pp.2 – 481. 2012.

[15] Y. W. 1. W. H. 1. J. Z. 2. a. X. W. 1. Xinfeng Li 1, "Effect of Surface Roughness on Hydrogen-Induced Blister Behavior in Pure Iron," Metals, vol. 10, no. 745, 2020.